Preparation of metal-organic frameworks with bimetallic linkers and corresponding properties

Dongdong Huang[1,2], Yi Liu[2], Yongfeng Liu[2], Duolong Di[2*], Hao Wang[2], Wu Yang[1*]

1. College of Chemistry and Chemical Engineering, Northwest Normal University, Lanzhou 730070, PR China
2. CAS Key Laboratory of Chemistry of Northwestern Plant Resources and Key Laboratory for Natural Medicine of Gansu Province, Lanzhou Institute of Chemical Physics, Chinese Academy of Sciences (CAS), Lanzhou 730000, PR China

*Corresponding authors, E-mail: didl@licp.cas.cn, xbsfda123@126.com

Characterization

X-ray diffraction (XRD) was recorded in the 2θ range of 2°~80° with Cu Kα radiation (λ=1.5418 Å) using a D/max-2500 diffractometer (Rigaku Corp., Japan). The surface morphology of the MOFs material was observed by a scanning electron microscope (SEM, Zeiss, ULTRA Plus, Germany). Sputter the material with the gold coating before observation. Thermogravimetric analysis (TGA) was performed under a nitrogen atmosphere using a Perkin-Elmer DETLASERLES TGA7 thermogravimetric analyzer. The temperature was set from room temperature to 1073 K and the heating rate was 283 K/min. UV-Vis spectra were obtained on a dual-beam UV-Vis spectrophotometer from Procalix TU-1901 (Beijing General Analytical Instrument Co., Ltd). The results of the corresponding characterization mentioned above could be seen in Figs. S1-9.

UV-vis spectral analysis

The UV-vis spectra of BDC and the prepared MOFs materials were tested by UV-vis diffuse reflectance spectroscopy, as shown in Fig. S1. It can be seen that the two characteristic peaks of BDC were at around 264 and 310 nm. The characteristic peaks of MIL-53(Al) were at 224, 256 and 290 nm and MIL-53(Al) exhibited almost no absorption in the visible region, which was similar to a previous report[1]. It was found that MIL-53(Fe) exhibited strong absorption bands in the range of 200-600 nm. The characteristic absorption peaks were at about 228 and 500 nm, which may be ascribed to absorption induced by ligand-to-metal charge transfer (LMCT) of O(II) to Fe(III)[2]. It can be also seen that MIL-53(Fe) exhibited strong absorption in the visible region. However, the MIL-53(Fe, Al) exhibited a characteristic peak at 225 nm, which was close to the first characteristic peak of MIL-53(Al), and it showed no absorption in the visible region. The analyses above showed that the band gap energy of the three MOFs material was different from each other, indicated the MOFs materials were successfully prepared.

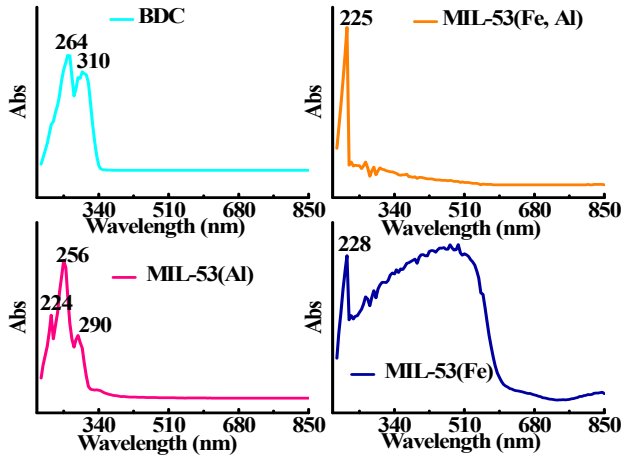

Fig. S1 UV-vis spectra of BDC and the prepared MOFs materials.

FTIR spectra analysis

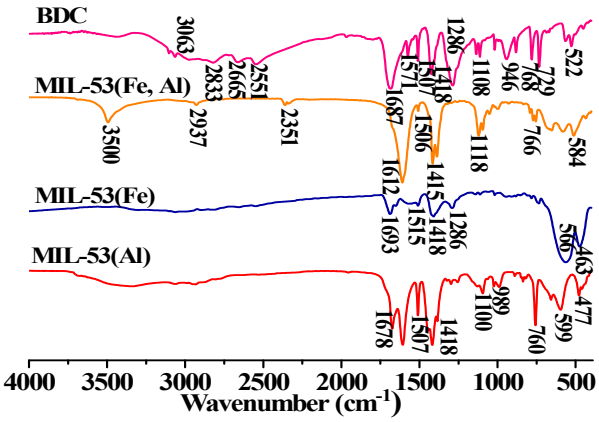

Fig. S2 FTIR spectra of BDC and the prepared MOFs materials.

FTIR spectra of BDC and the synthesized MOFs materials were shown in Fig. S2. The absorption bands at 1687, and 1507 cm^{-1} (were ascribed to the asymmetric stretching vibration of the carboxyl group of BDC and the absorption band at 1418 cm^{-1} was assigned to symmetric stretching vibration of carboxyl group[3-6]. The peaks at 1687 and 1507 cm^{-1} respectively shifted to 1693 and 1515 cm^{-1} in MIL-53(Fe), 1612 and 1506 cm^{-1} in MIL-53(Fe, Al), and 1678 and 1507 cm^{-1}in MIL-53(Al). In addition, the band at 768 cm^{-1} resulted from aromatic ring deformation shifted to smaller wavenumbers in the synthesized materials (766 cm^{-1}) in MIL-53(Fe, Al), MIL-53(Fe), and 760 cm^{-1} in MIL-53(Al) and the intensity remarkably changed. Furthermore, the spectra of MIL-53(Al) was similar to MIL-53-(2) of our previous report[6]. The presence of absorption band at 566 cm^{-1} of MIL-53(Fe) (599 cm^{-1} of MIL-53(Al), 584 cm^{-1} of MIL-53(Fe, Al)) suggested the vibration of metal-oxo bond

formation which was formed between the carboxylic group of BDC and the Fe(III) or Al(III)[5, 7]. The information mentioned above indicated that the MOFs materials were successfully prepared.

In addition, the infrared before and after adsorption showed in Fig. S3 and Fig. S4 of the materials MIL-53(Al) and MIL-53(Fe), were similar to the adsorption of glutathione by MIL-53(Fe, Al) in the paper.

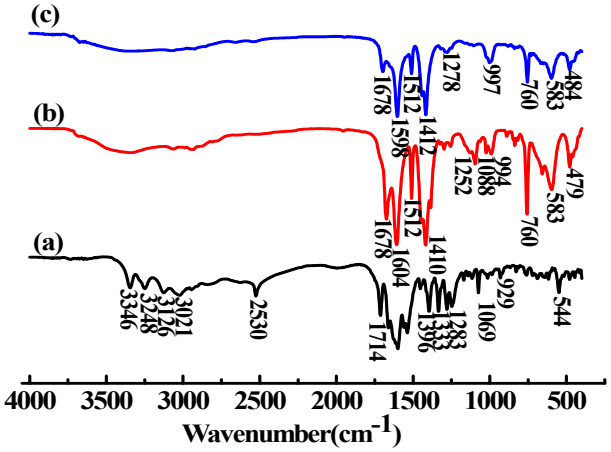

Fig. S3 FTIR spectra of (a) glutathione, (b) MIL-53(Al) and (c) glutathione loaded MIL-53(Al).

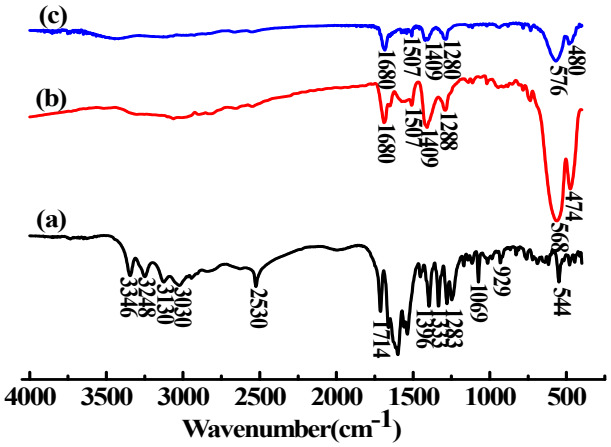

Fig. S4 FTIR spectra of (a) glutathione, (b) MIL-53(Fe) and (c) glutathione loaded MIL-53(Fe).

XRD analysis

The XRD patterns of MIL-53 (Fe, Al), MIL-53 (Fe) and MIL-53 (Al) were shown in Fig. S5. It can be seen that MIL-53(Fe) showed some strong diffraction peaks at 24.1°, 33.1°, 35.6°, and 40.1°, indicating the material had good crystallinity. But the pattern was not consistent with those reported[8,9], indicating the structure may be different due to different synthesized method. The materials in this study were prepared by a facile reflux method while MIL-53(Fe) reported in the references were prepared through a mild solvothermal process. However, the diffraction peaks of MIL-53 (Al) at 8.6°, 15.1°, 24.6°, 32.9°, 41.2° were in good agreement with the reference result[9,10,11], suggesting the successful formation of this material. Compared with MIL-53(Al), MIL-53(Fe, Al) only displayed some weaker peaks, indicating it possessed relatively poor crystallinity. However, the presence of two characteristic peaks at 33.1° and 35.6° exhibited that the MIL-53(Fe, Al) has been successfully

prepared.

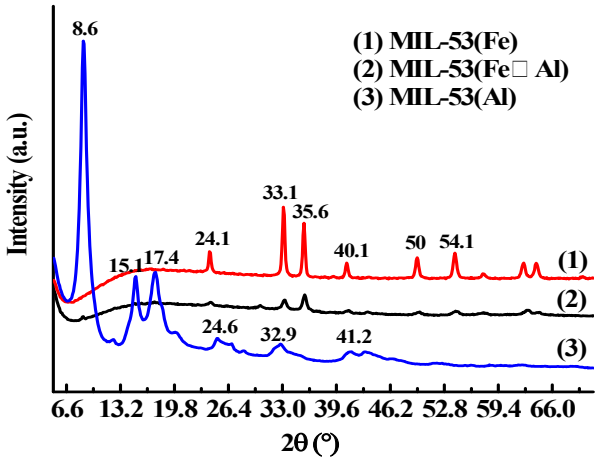

Fig. S5 XRD patterns of the prepared MOFs materials.

Thermogravimetric analyses

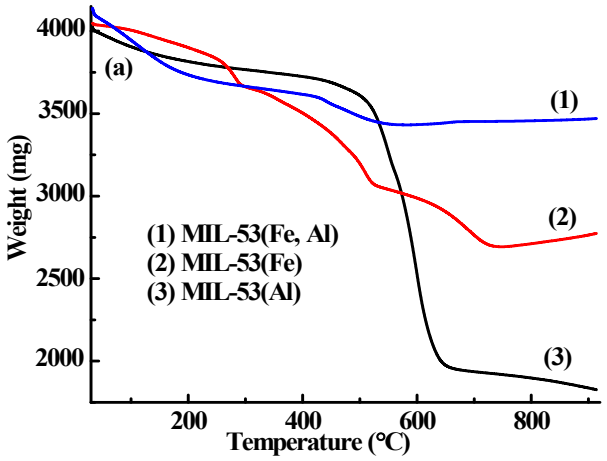

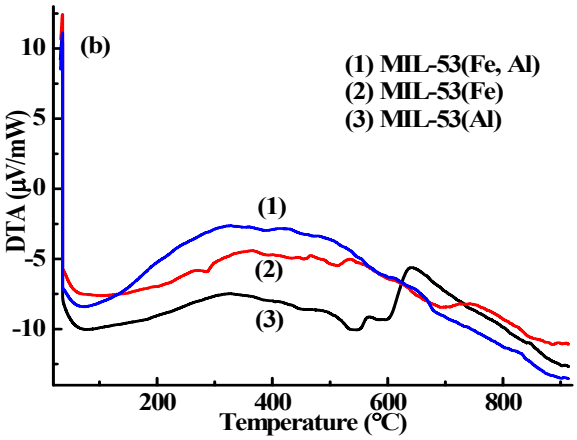

Fig. S6 (a) TGA curves and (b) DTA curves.

The TGA and DTA curves of MIL-53(Fe, Al), MIL-53(Fe) and MIL-53(Al) were shown in Fig. S6. The weight loss before 300 °C for the three MOFs materials was ascribed to the removal of water molecules adsorbed[12]. MIL-53(Al) was stable up to about 460 °C as the framework collapsed because of the elimination of BDC linkers from the framework resulting in the formation of Al_2O_3[3], while MIL-53(Fe, Al) was stable up to about 420 °C and the weight of MIL-53(Fe) was reduced after 300 °C, indicating the thermal stability of the three MOFs materials were different from each other. The shape of the TGA curve of MIL-53(Fe) was similar to a previous report[9]. The thermal stability was in the order of MIL-53(Fe) < MIL-53(Fe, Al) < MIL-53(Al). The residues were mainly inorganic matter and the weight of residues was in the order of MIL-53(Al) < MIL-53(Fe) < MIL-53(Fe, Al). The difference in thermal properties may hint the difference in corresponding structures, leading to different adsorption properties for glutathione. The DTA curve of MIL-53(Fe) was similar to that of MIL-53(Fe, Al), while the DTA curve of MIL-53(Al) was different from the other two MOFs materials, which was in line with the analyses of TGA curves.

Rheological properties

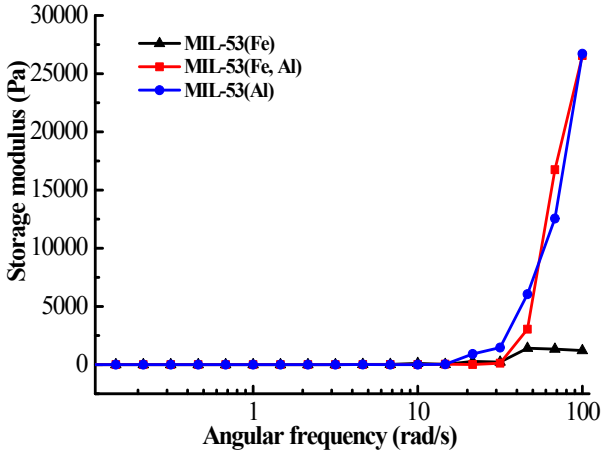

Fig. S7 The relationship between storage modulus and angular frequency.

In order to evaluate the mechanical properties of the prepared MOFs materials, rheological properties were studied in aqueous ethanol, and the relationship between storage modulus and angular frequency was shown in Fig. S7. It can be obviously seen that the storage modulus of the prepared MOFs materials remained unchanged and overlaps each other until the angular frequency is 20 rad/s. As the angular frequency exceeded to 20 rad/s, the storage modulus rapidly increased except MIL-53(Fe), and the storage modulus of MIL-53(Al) was close to that of MIL-53(Fe, Al) with angular frequency increasing, indicating the mechanic strength of MIL-53(Al) was similar to that of MIL-53(Fe, Al) and that of MIL-53(Fe) was weakest. It was may be due to the reaction between Fe(III) and carboxyl group was weaker than that

between Al(III) and a carboxyl group, leading to a difference in storage modulus[13].

SEM images

The microstructures of MIL-53(Fe), MIL-53(Al) and MIL-53(Fe, Al) were investigated, as shown in Fig. S8. MIL-53(Fe) displayed a polyhedral or small pseudo-spherical structure, which was similar to a previous report[8] (Fig. S6 (a)).For MIL-53(Al), it exhibited a rodlike structure and the rodlike particles were tended to aggregate together and form a big sphere(Fig. S6 (b)). However, MIL-53(Fe, Al) showed a large pyramid structure with a length of several micrometers, which was similar to the previously reported observation of MIL-53(Fe)[14] (Fig. S6 (c)). The morphology of the three MOFs materials was different from each other, indicating corresponding structures were different.

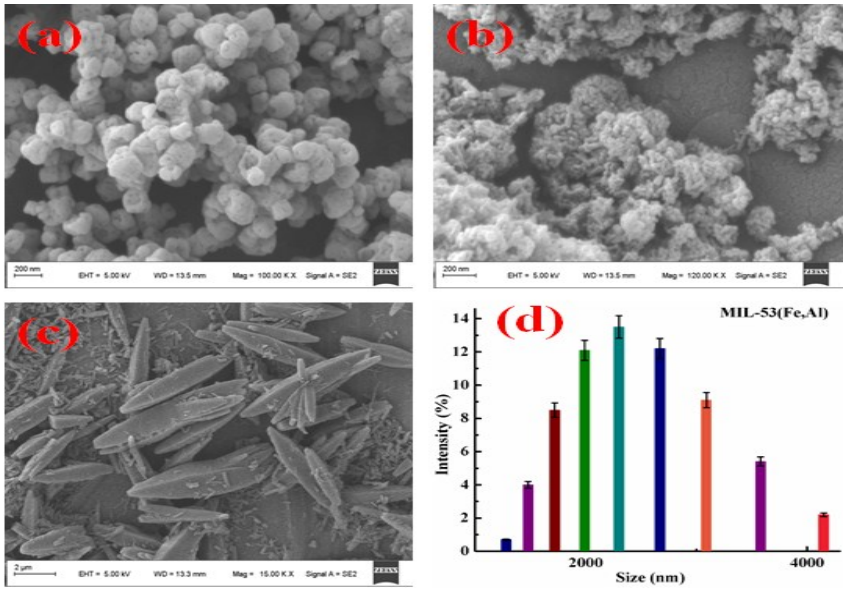

Fig. S8 (a) SEM image of MIL-53(Fe), (b) SEM image of MIL-53(Al), (c) SEM image of MIL-53(Fe, Al), and (d) particle size distribution of MIL-53(Fe, Al).

Nitrogen adsorption-desorption isotherms and pore size distribution

The surface area and porous structure of MIL-53(Al), MIL-53(Fe, Al) and MIL-53(Al) were measured by N_2 adsorption-desorption isotherms at 77 K, as shown in Fig. S9(a). At lower relative pressure, the nitrogen adsorbed increased sharply, indicating a high affinity for N_2, and as the relative pressure was in the range of 0.4 to 0.8, hysteresis loop appeared, suggesting the existence of mesopores and micropores in MIL-53(Fe, Al)[15, 16]. The BET surface area and total pore volume were computed to be in Table 3. From the pore size distribution in Fig. S9(b), it can be seen that the pores of MIL-53(Fe, Al) mainly lied in the range of 2 to 5 nm and the pore size distribution was narrow. The average pore width of MIL-53(Fe, Al) was 6.51 nm, which was calculated according to 4V/A by BET, and on the basis of Fig. S8(b), the pores of the MOFs materials were mainly mesopores and the BJH mesopore size distribution curve had a pore width centered at about 3.8 nm. MIL-53 (Al) adsorbed the amount of N_2 with increasing pressure over the entire pressure range. The sharp

increase in the amount of N_2 adsorbed can be observed as the pressure in the range of 0.6-1.0. The phenomenon indicated that the material MIL-53(Al) mainly contained mesoporous and microporous structure[17]. The adsorption amount of MIL-53(Fe) for N_2 was almost constant with the increase of pressure, while the pressure was in the range of 0.8-1.0, the pressure adsorption of MIL-53(Fe) for N_2 increases slowly[18]. Meantime, there was no hysteresis loop indicating no capillary evaporation. It can be seen that a mesoporous structure mainly contained in the material of MIL-53(Fe). The BET surface area and pore volume of the three MOFs materials were calculated, as shown in Table 3. BET surface area was in the order of $S_{MIL\text{-}53(Al)}>S_{MIL\text{-}53(Fe,\ Al)}>S_{MIL\text{-}53(Fe)}$, average pore width of $D_{MIL\text{-}53(Fe)}>D_{MIL\text{-}53(Fe,\ Al)}>D_{MIL\text{-}53(Al)}$ and Pore volume of $V_{MIL\text{-}53(Al)}>V_{MIL\text{-}53(Fe,\ Al)}>V_{MIL\text{-}53(Fe)}$. The BET surface area of the three materials is exactly the same as the order of the pore volume.

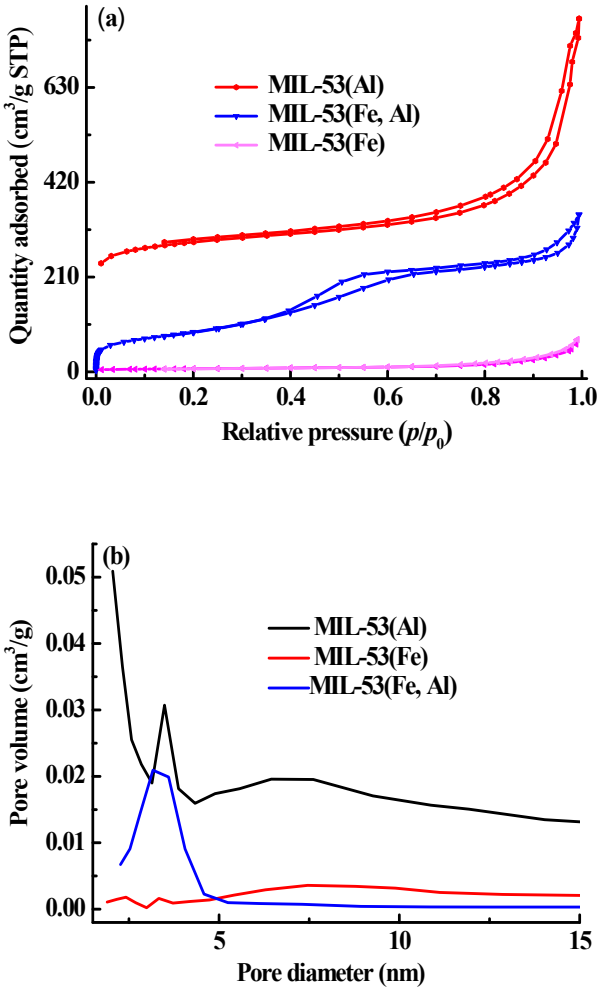

Fig. S9 (a) Nitrogen adsorption-desorption isotherms of the MIL-53(Al), MIL-53(Fe, Al) and MIL-53(Fe), (b) pore width distribution of the MIL-53(Al), MIL-53(Fe) and MIL-53(Fe, Al).

References

[1] D. Guo, R. Wen, M. Liu, H. Guo, J. Chen, W. Weng, Facile fabrication of g-C_3N_4/MIL-53(Al) composite with enhanced photocatalytic activities under visible-

light irradiation, Applied Organometallic Chemistry, 29 (2015) 690-697.
[2] Y. Fu, D. Sun, Y. Chen, R. Huang, Z. Ding, X. Fu, Z. Li, An amine-functionalized titanium metal-organic framework photocatalyst with visible-light-induced activity for CO_2 reduction, Angewandte Chemie, 51 (2012) 3364-3367.
[3] T. Loiseau, C. Serre, C. Huguenard, G. Fink, F. Taulelle, M. Henry, T. Bataille, G. Ferry, A rationale for the large breathing of the porous aluminum terephthalate (MIL-53) upon hydration, Chemistry-a European Journal, 10 (2004) 1373-1382.
[4] K. Nakamoto, Infrared and Raman Spectra of Inorganic and Coordination Compounds, 1986.
[5] R. Liang, F. Jing, L. Shen, N. Qin, L. Wu, MIL-53(Fe) as a highly efficient bifunctional photocatalyst for the simultaneous reduction of Cr(VI) and oxidation of dyes, Journal of Hazardous Materials, 287 (2015) 364-372.
[6] Y. Liu, Y. Liu, H. Wang, L. Dong, D. Di, Preparation of metal‐organic frameworks hybridizing with attapulgite and adsorption behaviors for glutathione reduced, Journal of Chemical Technology & Biotechnology, (2018).
[7] C.R. Gong, D.R. Chen, X.L. Jiao, Q.L. Wang, Continuous hollow alpha-Fe_2O_3 and alpha-Fe fibers prepared by the sol-gel method, Journal of Materials Chemistry, 12 (2002) 1844-1847.
[8] L. Ai, C. Zhang, L. Li, J. Jiang, Iron terephthalate metal-organic framework: Revealing the effective activation of hydrogen peroxide for the degradation of organic dye under visible light irradiation, Applied Catalysis B Environmental, 148-149 (2014) 191-200.
[9] J.-J. Du, Y.-P. Yuan, J.-X. Sun, F.-M. Peng, X. Jiang, L.-G. Qiu, A.-J. Xie, Y.-H. Shen, J.-F. Zhu. New photocatalysts based on MIL-53 metal-organic frameworks for the decolorization of methylene blue dye, Journal of Hazardous Materials, 190 (2011) 945-951.
[10] C.-X. Yang, H.-B. Ren, X.-P. Yan, Fluorescent Metal-Organic Framework MIL-53(Al) for Highly Selective and Sensitive Detection of Fe^{3+} in Aqueous Solution, Analytical Chemistry, 85 (2013) 7441-7446.
[11] V. Finsy, L. Ma, L. Alaerts, D.E. De Vos, G.V. Baron, J.F.M. Denayer, Separation of CO_2/CH_4 mixtures with the MIL-53(Al) metal-organic framework, Microporous and Mesoporous Materials, 120 (2009) 221-227.
[12] S. Shahid, K. Nijmeijer, High-pressure gas separation performance of mixed-matrix polymer membranes containing mesoporous Fe(BTC), Journal of Membrane Science, 459 (2014) 33-44.
[13] Y. Cao, J. Zhang, J. Feng, P. Wu, Compatibilization of immiscible polymer blends using graphene oxide sheets, ACS Nano, 5 (2011) 5920-5927.
[14] Y. Gao, S. Li, Y. Li, L. Yao, H. Zhang, Accelerated photocatalytic degradation of organic pollutant over metal-organic framework MIL-53(Fe) under visible LED light mediated by persulfate, Applied Catalysis B-Environmental, 202 (2017) 165-174.
[15] G. Ji, Z. Yang, H. Zhang, Y. Zhao, B. Yu, Z. Ma, Z. Liu, Hierarchically Mesoporous o-Hydroxyazobenzene Polymers: Synthesis and Their Applications in

CO2 Capture and Conversion, Angewandte Chemie-International Edition, 55 (2016) 9685-9689.
[116] W. Kuang, Y.N. Liu, J. Huang, Phenol-modified hyper-cross-linked resins with almost all micro/mesopores and their adsorption to aniline, Journal of Colloid & Interface Science, 487 (2017) 31-37.
[17] J. Warfsmann, B. Tokay, N. R. Champness, Synthesis of Hydrophobic MIL- 53 (Al)-nanoparticles in Low Weight Alcohols: Systematic Investigation of Solvent Effects. Crystengcomm, 20 (2018) 4666-4675.
[18] W. P. Xiong, G. M. Zeng, Z. H. Yang, et al, Adsorption of tetracycline antibiotics from aqueous solutions on nanocomposite multi-walled carbon nanotube functionalized MIL-53(Fe) as a new adsorbent, Science of the Total Environment, 627 (2018) 235-244.